water

MDPI

Article

A Comparative Study of Comprehensive Modeling Systems for Sediment Transport in a Curved Open Channel

Keivan Kaveh *, Markus Reisenbüchler, Sandip Lamichhane, Tobias Liepert, Ngoc Dung Nguyen, Minh Duc Bui and Peter Rutschmann

Institute of Hydraulic and Water Resources Engineering, Technische Universität München, Arcisstraße 21, D-80333 München, Germany

* Correspondence: keivan.kaveh@tum.de

Received: 8 July 2019; Accepted: 23 August 2019; Published: 27 August 2019

Abstract: In recent decades, a variety of morphodynamic model systems have been developed to improve our understanding of sediment transport and the resulting changes in riverbed topography. Despite progress in the description of physical processes, the degree of accuracy of morphodynamic model results remains difficult to assess and are also less than for hydrodynamics alone. In this paper, three different 2D morphodynamic systems have been applied to simulate a complex hydrodynamic and morphodynamic situation. These model systems were validated using data of sediment sorting and bed deformation conducted in a 180° channel bend under unsteady-flow conditions. The calculations obtained by each modeling system were compared with the available observed data. The simulated results showed that all applied morphodynamic models could precisely calculate the bed level changes and the areas of deposition and scour. However, the models are not efficient enough to predict the distribution of the mean grain size in the channel bend.

Keywords: TELEMAC-MASCARET; HYDRO-FT; BASEMENT; alluvial curved channel; hydro-morphodynamics

1. Introduction

Rivers are present in nature in a variety of forms, such as straight, sinuous, meandering, and braided, because of interacting processes among water flow, sediment transport, and vegetation. Modeling of hydro-morphodynamics, also known as river morphodynamics, is vital to understand how the mentioned interacting processes work. The results can assist decision-making at multiple levels that can promote an environmentally friendly and cost-effective river basin and land management. However, modeling the complex interactions of hydro-morphodynamic processes are driven by various physical and numerical parameters, and many methods are reproduced using empirical formulations. Generally, several formulations for the same process (e.g., bed-load transport equation) exist. Most of these formulations employ an empirical relation for the equilibrium transport rate, which corresponds to the transport capacity of the flow, i.e., the bed material load discharge is equal to the sediment transport capacity of the flow. Further, sediment transport equations are equilibrium relationships based upon laboratory and field data collected under uniform flow conditions in shallow water bodies. The modeler must be aware of the limitations of these models to be able to reproduce the real behaviors of the river.

Determining the evolution of a given bed configuration due to the motion of the fluid and the resulting sediment transport was first examined in a theoretical context in a previous study [1]. Exner's work [1] in this area can be considered as a classical treatment of the problem and appears in many

texts [2–5]. His work proposes the conservation of sediment mass, and in the literature this is often referred to as the Exner equation, which is the foundation of estuarine and river morphodynamics. From equations for the conservation of fluid and sediment mass, and through several simplifying assumptions, Exner derives a simplified bed evolution model that takes the form of a nonlinear hyperbolic scalar equation. Despite the relative simplicity of this model, the results obtained are, to a limited extent, in good agreement with what is observed in nature. The analytical solution provided by Exner for his model is the so-called classical or genuine solution of the initial-value problem, which is valid while the solution is continuous [6].

Numerical morphological models also involve the coupling with a hydrodynamic model and an equation for bed level change. The sediment conservation equation is a physical nonlinear equation for the bed level similar to other mass conservation equations. A common feature of these conservation laws is shock waves. This means that discontinuities of the respective physical quantities will develop when particle velocity approaches celerity [7]. Several decades of research effort have been devoted to the development of numerical solution techniques to obtain an accurate and stable simulation of shock behavior, including the invention of shock-capturing methods. The methods can be classified into two general categories: classical and modern techniques. The well-known classical shock-capturing methods include the MacCormack method, Lax–Wendroff method, and Beam-Warming method. Examples of modern shock-capturing schemes include higher-order total variation diminishing (TVD) schemes, flux-corrected transport scheme, monotonic upstream-centered schemes for conservation laws (MUSCL) based on [8], and the piecewise parabolic method (PPM). Another important class of high-resolution schemes belongs to the approximate Riemann solvers from previous work [9]. Examples of such models are the work of previous authors [10–14].

Recent examples of studies on coupling 3D flow and morphodynamics can be found in the literature [15–21]. One previous study [15] employed a three-dimensional coupled hydro-morphodynamic model, the virtual flow simulator (VFS-Geophysics), in its unsteady Reynolds-averaged Navier–Stokes mode closed with the k-ω model to simulate the turbulent flow and sediment transport in large-scale sand and gravel bed waterways under prototype and live-bed conditions. The simulation results were used to carry out systematic numerical experiments to develop design guidelines for rock vane structures in curved channels. Another study [16] numerically investigated local scour around three real-life in-stream restoration rock structures. According to their work, the flow field is simulated by solving the unsteady Reynolds-Averaged Navier-Stokes (RANS) equations closed with the k-ω turbulence model. The bed evolution is calculated by solving the Exner equation using an unstructured, finite-volume formulation. Comparisons with measurements show that the computed results capture both the spatial and temporal features of scouring and deposition patterns with good accuracy. Another study [17] developed a numerical model to investigate the initial stages of erosion and the development of ripples produced by the turbulent horseshoe vortex system in the vicinity of a surface-mounted cylindrical pier. They simulated flow using the detached eddy simulation approach. To compute the erosion, the Exner equation was coupled to a new bed-load transport model that directly incorporates the effect of the instantaneous flow field on sediment transport. The morphodynamic model is integrated simultaneously with the flow equations using an arbitrary Lagrangian–Eulerian method for moving boundaries.

In the past decades, a variety of morphodynamic model systems have been developed to predict the natural and anthropogenic bed evolution in rivers, estuaries, and seas. However, it is still challenging to evaluate the accuracy of models in morphodynamic simulations. The choice of model parameters requires a significant degree of expertise from end-users to adapt the model to their application properly. ECOMSed [22], Mike-21 [23], Delft3D [24], ROMS [25], FAST3D (developed at the Institute of Hydromechanics, University of Karlsruhe, Germany), HYDRO-FT, TELEMAC-MASCARET, and BASEMENT are some examples of hydro-morphodynamic modeling systems, which generally include different flow modules (from 1D to 3D), a wave propagation model, and a sediment transport model, including bed-load and suspended load. Most existing morphodynamic modeling systems rely on finite difference methods, and are therefore constrained by the use of a boundary (orthogonal

curvilinear horizontal coordinate systems, sigma stretched vertical coordinates), making them only suitable for simplified geometry. Moreover, filtering methods, such as the lengthening of the tide or the use of the so-called morphodynamic factor [26], which have been extensively applied to reduce computational costs for long term applications, introduce an additional source of uncertainty [27]. On the other hand, most existing morphodynamic modeling systems rely on numerical methods, therefore having high computational costs for long-term applications.

In this paper, three comprehensive morphodynamic modeling systems, including HYDRO-FT, TELEMAC-MASCARET, and BASEMENT, have been applied to simulate complex hydrodynamic and morphodynamic situations in a curved channel. The complexity of such a simulation in a channel bend, which is due to two reasons, warrants this to be considered as the test case. Firstly, the highly non-uniform sediment in a channel bend is subject not only to longitudinal transport but also to transverse transport and transverse sorting by the secondary flow inherently associated with the curves. Secondly, the unsteadiness of flow in natural rivers certainly has some effects on the structure of the flow field, thereby affecting the motion of sediment particles. In the applications presented here, the sediment transport model is mainly restricted to the transport of non-cohesive sediments, which relies on classical semi-empirical concepts, including sand grading effects and parameterization of secondary current sand–wave effects. In order to evaluate the efficiency and accuracy of each model system, the simulation results are compared with measured bed topography and sediment sorting in the channel bend obtained in the laboratory in a previous study [28].

2. Morphological Model Systems

2.1. TELEMAC-MASCARET

The open-source TELEMAC-MASCARET was developed originally by the National Hydraulics and Environment Laboratory (LNHE) of the research and development directorate of the French Electricity Board (EDF) as a hydro-informatics system for free surface flows [29]. All modules of the system are based on unstructured grids and finite element or finite volume algorithms. One crucial feature is parallelism with domain decomposition. The implicit algorithms have led to a partitioning without overlapping, with matching interface points, and linear systems solved over the whole domain. The programs are written in Fortran 90 and can be run on Unix, Linux, and Windows systems; they are compatible with any Fortran 90 compiler. The model system includes 2D and 3D hydrodynamic modules (TELEMAC-2D and -3D), and a spectral wave propagation model called "TOMAWAC". The environment is extended by the two-dimensional morphologic module called "SISYPHE" for bed-load and depth-averaged suspended load and SEDI-3D for the three-dimensional suspended load. More detailed information about the system can be found on the website: http://www.opentelemac.org/.

2.1.1. Hydrodynamic Module

The TELEMAC-2D flow module solves the Shallow Water Equations (SWE) with several options for the horizontal dispersion terms (e.g., depth-averaged k-ε model, Elder model, and constant eddy viscosity models) and source terms (e.g., atmospheric pressure gradients, Coriolis force). The numerical discretization includes a choice of classical methods for the advection terms (e.g., characteristics, Streamline-Upwinded Petrov-Galerkin (SUPG), distributive schemes). The use of implicit schemes allows for time step limitations to be relaxed (typically, values of a Courant-Friedrichs-Lewy number (CFL) up to 10 or 50 are acceptable). Recently, ideas stemming from finite volume techniques have been coupled with these implicit schemes to ensure monotonicity of depth and sediment concentrations, as well as mass conservation of machine accuracy.

TELEMAC-3D solves the Reynolds-averaged Navier–Stokes (RANS) equations in unstructured meshes obtained by a superimposition of 2D meshes of triangles. The movement of the mesh can be considered in the advection step by the transformation. The superimposed layers may not be evenly spaced. This allows a more accurate representation of the flow field by a refinement near the bed,

enabling better accuracy of the turbulence models (mixing-length model, k-ε model) and leading to a better estimate of the bed shear stress. The 3D model can be applied to capture the effect of vertical recirculation cells as well as stratification effects, assuming a hydrostatic or non-hydrostatic pressure distribution [30].

2.1.2. Sediment Transport and Morphodynamic Module

Sediment transport and bed change module (SISYPHE) can be used to model complex morphodynamic processes for different flow conditions, sediment size classes, and sediment transport modes. In SISYPHE, sediment transport processes are grouped as bed-load, suspended load, or total-load, with an extensive library of bed-load transport relations. Differing sediment transport formulae for bed-load or total-load are implemented. SISYPHE is applicable to non-cohesive sediments that can be uniform or non-uniform, as well as cohesive sediments and sand-mud mixtures. Several physically based processes are incorporated into SISYPHE, such as the influence of secondary currents to precisely capture the complex flow field induced by channel curvature, the effect of bed slope associated with the influence of gravity, bed roughness predictors, and areas of the non-erodible bed, among others. SISYPHE can be coupled to the depth-averaged shallow water module TELEMAC-2D or the three-dimensional Reynolds-averaged Navier–Stokes module TELEMAC-3D. The sediment transport model relies on a complete description of the flow field through internal coupling with the flow module. At each time step, the hydrodynamic model (TELEMAC) calculates the flow field and sends the spatial distribution of the main hydrodynamic variables (water depth, flow velocity components, and bed shear stress) to the SISYPHE model. These sediment transport rates are calculated and bed level change is used to account for the effects of sediment transport on flow. The structure of such a coupled system is shown in Figure 1.

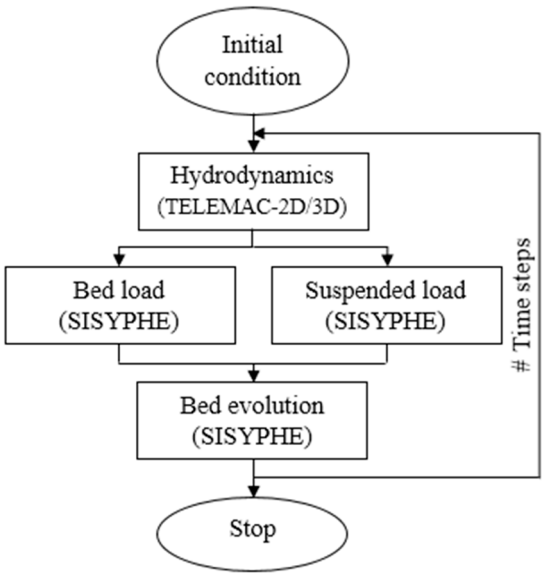

Figure 1. Scheme of a hydro-morphodynamic model system.

Sediment transport rates in the modeling system are calculated with classical semi-empirical concepts, which involve the decomposition of sediment transport rates into bed-load and suspended load. The resulting bed evolution is then computed by solving Exner's equation. The model is mainly applicable to non-cohesive sediment composed of either uniform grains or multi-grains and characterized by their mean size and density. The conventional method for performing hydro-morphodynamic simulations in rivers is to decouple the hydrodynamic and the morphodynamic modules. The decoupling approach is based on the rationale that the channel bed reacts at a much slower timescale than the flow. At the implementation level, these modules communicate through a quasi-steady morphodynamic time-stepping mechanism. During flow computation, the bed level is assumed to be constant, and during

computation of the bed level, the flow and sediment transport quantities are assumed invariant to the bed level changes. The modules are linked together at the programming level.

2.2. HYDRO-FT-2D

HYDRO_FT-2D is a software system that enables simulating two-dimensional sediment transport processes. It was developed as an add-on to the hydraulic flow simulation system HYDRO_AS-2D. Apart from flow equations, equations pertaining to the concentration of suspended material and streambed alteration (Exner equation) are solved numerically.

2.2.1. Hydrodynamic Module

Two-dimensional hydrodynamic numerical simulation model, named HYDRO_AS-2D, was mainly developed for the calculation of dam break and flood wave propagation. Nevertheless, it can be successfully used in common two-dimensional flow simulations. In addition to the main program, which strictly performs hydrodynamic calculations, there are modules for the calculation of suspended load and bed-load transport (FT) and heat transfer (WT). The hydrodynamic module is based on the shallow water equations. As a result, when the vertical flow velocity component plays an essential role, a vertical layer model of a three-dimensional simulation model would be appropriate. Hence, the range of applicability of HYDRO_AS-2D is closely related to the question of problem dimensionality. Fortunately, previous experience shows that many practical problems of water engineering can be successfully described with the depth-averaged flow equations. Even complex flow conditions in flooded river valleys can be simulated effectively [31–34].

HYDRO_AS-2D uses a numerical mesh composed of triangular and rectangular elements. This type of mesh enables a simple adaptation to specific topographic and hydrodynamic conditions of each problem. This allows for intuitive and precise modeling of the river course, dikes, and road embankments, all of which are vital for a realistic presentation of flow processes.

The finite volume approach is known for its conservative properties, which make is very suitable for the calculation of discontinuous sections (e.g., hydraulic jumps, sudden changes in bed level, and widening or constriction of the channel width). Due to those conservative properties mass losses do not occur, as opposed to some other approaches.

2.2.2. Sediment Transport and Morphodynamic Module

The following modules exist as add-ons to HYDRO_AS-2D for sediment transport and morphodynamic simulations. GS1 is a bed-load transport module for only one fraction, GSm is a bed-load transport module for up to 12 fractions, ST is a solvent transport module for up to 12 fractions, and FT is a bed-load and solvent transport for up to 12 fractions. The part of the program enabling the simulation of up to 12 fractions was been with Hunziker, Zarn, and Partner S.G. The stream bed alteration, which is due to the sediment erosion and sedimentation of suspended material and bed-load, can be determined fractionally (Exner equation). The cumulative stream bed alteration is calculated as the sum of the fractionated stream bed alteration. The sediment consists of several layers that are managed following a program routine [35]. Figure 2 roughly illustrates the interchanging processes between sediment layers.

In the following, the interchanging processes between the active layer and sub-layer due to erosion and sedimentation of the stream bed are summarized (see Figure 3).

For erosion:

- If the critical bed shear stress is exceeded, the stream bed erodes, and material is removed from the active layer.
- By definition thickness of the active layer (h_AL) is unchangeable. Consequently, the material is transferred from the sub-layer to the active layer to compensate for the erosion.

- In the case of a multi-grain setup, median grain diameter (dm_AL) and mass portion per grain fraction (FA_AL-i) in active layer change due to the material influx from the sub-layer.
- Here, thickness of sub-layer (h_UL) decreases due to the material discharge, while median grain diameter (dm_UL) and mass portion per grain fraction (Fa_UL-i) in sub-layer remain unchanged. If the minimum sublayer thickness is reached, the basic layer erodes.
- During erosion of the basic layer, the sub-layer adopts the constantly changing composition of the basic layer: dm_UL = dm_BL (median grain diameter in basic layer), and FA_UL-i = FA_BL-i (mass portion per grain fraction in basic layer).

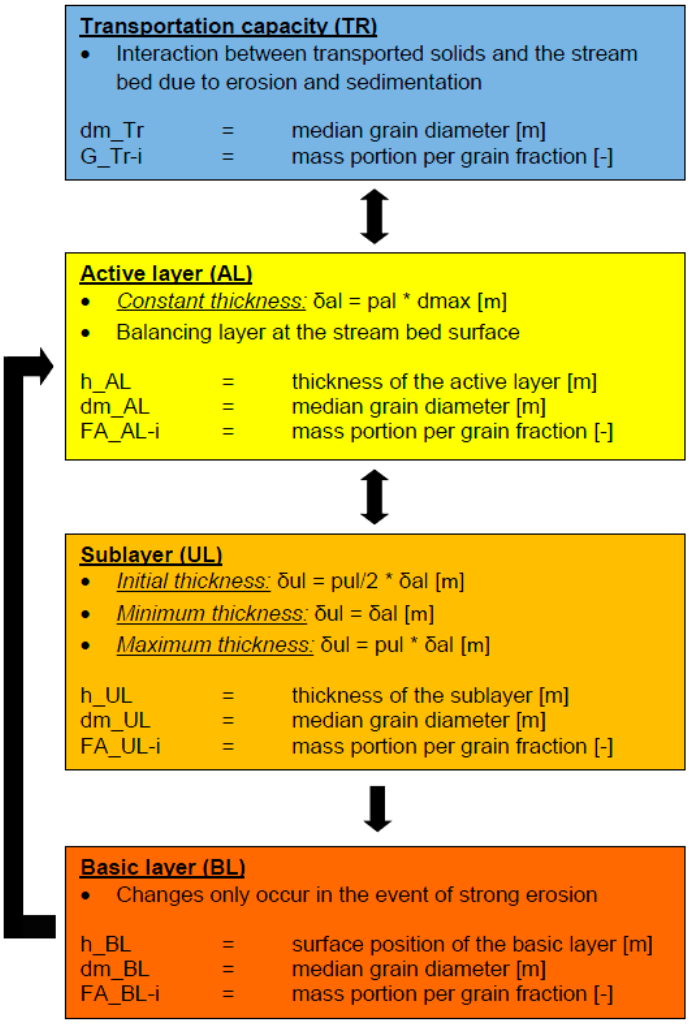

Figure 2. Sediment layers in HYDRO_FT-2D.

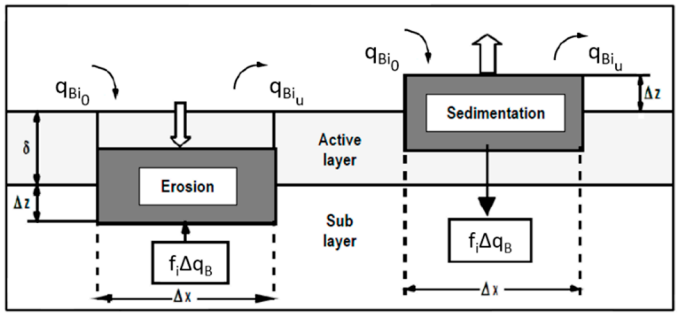

Figure 3. Model concept of an active layer according to Hirano.

For Sedimentation:

- Multiple factors, such as low flow velocity, can cause sedimentation, which leads to the material influx to the active layer.
- By definition h_AL is unchangeable. Consequently, the material is transferred from the active layer to sub-layer to compensate for the sedimentation.
- In the case of a multi-grain setup, dm_AL and FA_AL-I change due to the deposited material, h_UL increases due to material flow from the active layer to sublayer, dm_UL, and FA_UL-i alter.
- If the maximum sublayer thickness is reached, the material is transferred from the sub-layer to the basic layer. Surface portion of the basic layer (h_BL) increases median grain diameter in basic layer (dm_BL), and FA_BL-i alter.

2.3. BASEMENT

Basic Simulation Environment for Computation of Environmental Flow and Natural Hazard Simulation (BASEMENT) was developed at the Laboratory of Hydraulics, Hydrology, and Glaciology, Eidgenössische Technische Hochschule (ETH) Zurich. It offers a flexible Graphical User Interface (GUI) and functional environment for numerical simulation of alpine rivers and sediment transport. The software is mainly comprised of the one-dimensional and two-dimensional flow computation with moving boundaries and an appropriate model for bed-load as well as a suspended load. It focuses on the stability of numeric models, the flexibility of the computational grid, and the combination and efficiency of the calculation method. The core of BASEMENT consists of numerical solution algorithms comprised of the appropriate modules. Pre- and post-processing are done with independent products using a well-defined common interface [36]. Figure 4 shows the complete system overview of BASEMENT. The BASEchain module deals with the 1D flow, whereas BASEplane module deals with the 2D flow.

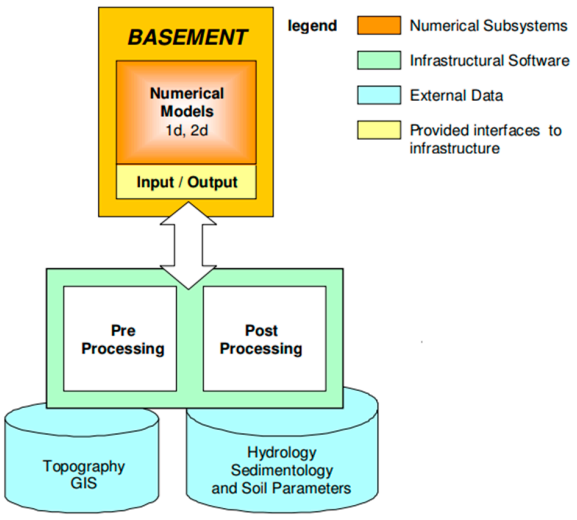

Figure 4. BASEMENT system overview.

2.3.1. Hydrodynamic Module

In the BASEMENT modeling system, the behavior of fluid hydraulics is explained with physical models, namely the conservation of mass and momentum. Theoretically, it is possible to resolve the mathematical problem for small scale phenomena, such as turbulence structures. In a natural problem, however, it is mostly impossible to determine all boundaries and the exact initial conditions. Furthermore, the computational time needed to solve the full system of equations is rapidly increasing with higher spatial and temporal resolution. Therefore, dependent on the problem, the BASEMENT uses simplified mathematical models. In three dimensions, the flow and pressure distribution are completely described by the Navier–Stokes equations. These equations can only be solved numerically,

as analytical solutions only exist for some overly simplified problems. The 3D approach is only suitable for local problems where turbulence phenomena and flow in all directions are essential for the results, e.g., the flow around bridge piers.

Supposing that the vertical velocity acceleration of water particles is negligible, integration over the flow depth is allowed, which results in the shallow water equations. They form a time-dependent, two-dimensional system of non-linear partial differential equations of the hyperbolic type. This set of equations provides accurate results for the behavior of water levels and velocities in a plane. Turbulence effects cannot be resolved anymore but are accounted for by an artificial friction factor in the closure condition, which establishes a relation between flow velocity and shear stress. The shallow water equations are used for 2D flows, such as dam breaks and curved flow. The main outputs of these equations are the water level and mean velocity in the flow direction. This method is still in use for computing large river systems.

2.3.2. Sediment Transport and Morphodynamic Module

The mathematical computation of sediment transport is not as well-developed as the hydrodynamic part. Theoretically, the movement of every single stone within the sediment could be computed by solving its equation of motion; however, this approach is still numerically too expensive. Therefore, sediment transport and behavior of the riverbed are calculated using empirical formulas developed by river engineers. The computation of the sediment flux is not physically correct but has proved to be accurate enough for a broad range of sediment transport problems. Usually, sediment transport occurs in the main flow direction. More sophisticated models also consider lateral phenomena within a curved flow. Very small grain sizes are treated as suspended sediment load, and their behavior can be computed by a physically scalar transport equation.

In more detail, the sediment transport equations are solved by vertical and spatial discretization. The finite volume method is applied to discretize the morphodynamic equations. Figure 5 shows the numerical model with a vertical partition into three main control volumes: the upper layer for momentum and suspended sediment transport, the active layer for bed-load sediment transport as well as bed material sorting, and the sublayer for sediment supply and deposition. The primary unknown variables of the upper layer are water depth h and specific discharge q and r in the directions of Cartesian coordinates x and y. Here, $q_{Bg}.x$ and $q_{Bg}.y$ describe the specific bed-load fluxes of the active layer. The bed level change Z_B is obtained through combinations of balanced equations for water and sediment and the corresponding exchange terms (e.g., bed slope, bottom friction) between the vertical layers.

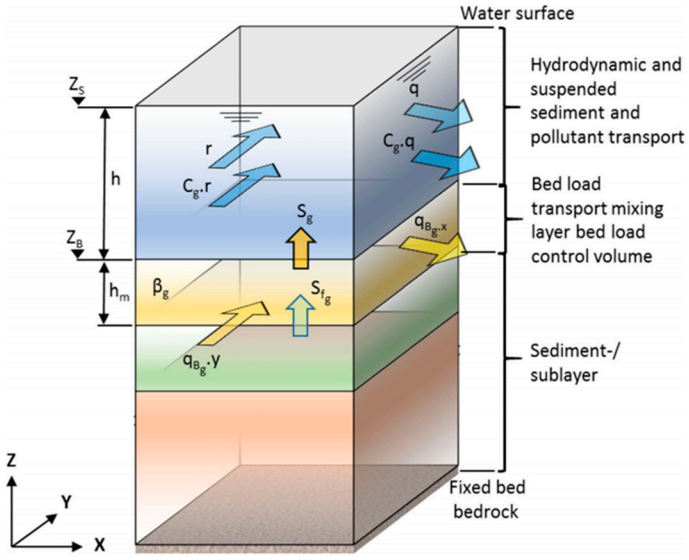

Figure 5. Vertical discretization of a computational cell in the BASEMENT system.

2.4. Background and Application Range of Modeling Systems

As mentioned in Section 2.2, HYDRO_FT-2D was developed as an add-on to HYDRO_AS-2D, which is hydraulic flow simulation system. HYDRO_AS-2D was mainly developed for the calculation of dam break and flood wave propagation. Nevertheless, it can be used successfully for common two-dimensional flow simulations. It can be said that HYDRO_FT-2D is oriented for an engineering problem. On the contrary, the open TELEMAC-MASCARET is a mathematically superior suite of solvers for use in the field of free-surface flow. Having been used in the context of many studies throughout the world, it has become one of the major standards in its field. The main application of TELEMAC-2D is in free-surface maritime or river hydraulics; however, the software has many fields of application. The program is able to consider many phenomena, such as propagation of long waves with non-linear effects, turbulence, coupling with sediment transport, wave-induced currents, treatment of singularities, and dry areas in the computational field. In the maritime sphere, particular mention may be made of the sizing of port structures, the study of the effects of building submersible dikes or dredging, the impact of waste discharged from a coastal outfall, or the study of thermal plumes. In river applications, studies on the impact of construction works (bridges, weirs, tubes), dam breaks, flooding, or the transport of decaying or non-decaying tracers can be mentioned. TELEMAC-2D has also been used for a number of special applications, such as the bursting of industrial reservoirs and avalanches falling into a reservoir. In the case of BASEMENT, the key features of the software are 2D hydro- and morphodynamics, slope collapse, model coupling, and automatic control.

Table 1 summarizes important background information on physical and mathematical theories, as well as numerical methods available in each modeling system. As can be seen from this table, the TELEMAC modeling system supports 3D RANS hydrodynamic simulations, whereas, the two other models are only capable of 2D hydrodynamic simulations. In HYDRO-FT and BASEMENT modeling systems, there is only one turbulence model available, while TELEMAC offers the user six options of different complexity, such as constant viscosity, Elder model, and k-ε model. For sediment transport modeling, the BASEMENT model provides a wide range of bed-load formulae, which makes its use more flexible for transport modeling. The transport of sediment materials can be calculated with only three equations in HYDRO-FT. In TELEMAC-MASCARET, the user is able to choose between either finite volume method (FVM) or finite element method (FEM) for hydrodynamic numerical simulation, while HYDRO_FT and BASEMENT use only the finite volume method for solving flow equations. In TELEMAC, finite elements resolution is based on the primitive equations. It is possible to replace the original equations with a generalized wave equation obtained by eliminating the velocity from the continuity equation using a value obtained from the momentum equation. This technique increases calculation speed but has the disadvantage of smoothing the results. When using the finite volume scheme, the primitive equations written in the conservative form are solved using seven different types of schemes. The available possibilities for each modeling system are listed in Table 1. These include Harten-Lax-van Leer (HLL), Harten-Lax-van Leer-contact (HLLC), and weighted average flux (WAF) schemes. Both HYDRO-FT and BASEMENT modeling systems have the capability to perform simulation-based structured and unstructured meshes, whereas TELEMAC is only based on unstructured mesh grids. More detailed information about the physical and mathematical theories behind each modeling system can be found in the user manual for the software.

Table 1. Background information on physical and mathematical theories, as well as numerical methods applied in each modeling system.

Physical and Mathematical Model	Modeling System			
	TELEMAC-MASCARET		HYDRO-FT	BASEMENT
Hydrodynamic Models	2D: Saint-Venant FEM, Saint–Venant FVM, Boussinesq	3D: RANS	2D: SWE	2D: Boussinesq
Turbulence Models	Constant viscosity, Elder, k-ε model, Smagorinski, mixing length, Spalart–Allmaras		combination of an empirical viscosity and constant viscosity	Boussinesq eddy viscosity
Sediment Transport Models	Bed-load formula: Meyer–Peter, Einstein–Brown, Engelund–Hansen, Bijker, Van Rijn, Hunziker, Bailard, Dibajnia et Watanabe		Bed-load formulae: Meyer–Peter and Müller (MPM), Engelund–Hansen, Ackers–White	Bed-load formula: Meyer–Peter and Müller (MPM), Engelund–Hansen, Hunziker, MPM extended by Ashida and Michiue, Ashida and Michiue, Parker, Wilcockcrowe, Power law, Rickenmann, Smart and Jaeggi, Smart and Jaeggi extended for Ashida and Michiue, Wu, Van Rijn
Numerical Methods	FVM scheme: Roe, HLLC, WAF Kinetic order 1, Kinetic order 2, Zokagoa, Tchamen	FEM scheme: Multiple schemes for advection of velocity, tracer, k-ε	FVM scheme: First and second-order explicit Runge–Kutta	FVM scheme: Godunov type methods, HLL, HLLC
Mesh	Unstructured		Structured/ Unstructured	Structured/ Unstructured

3. Validation Test Case

The laboratory experiments conducted in previous work [28] in 180° channel bends with the radius of curvature along the central bend line (r_c) for 4 m with width (B) of 1 m has been considered to validate the applied model systems. The bends had stilling basins of 11.5 m lengths on the upstream side and a sediment-settling tank on the downstream side of the same length, as shown in Figure 6.

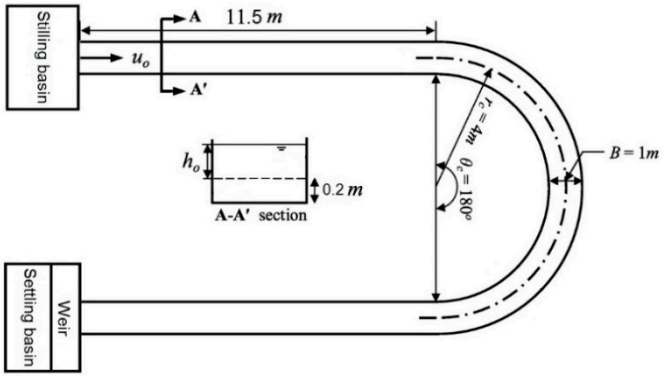

Figure 6. Bend channel geometry.

A 0.2-m thick sand layer had a sediment of median diameter and standard deviation (d_{50}) of 0.001 m and 2.5, respectively. The sand was classified into eight-grain sizes (see Table 2) and laid carefully with the desired gradation. They maintained the initial slope of 0.002 with the help of two

rails supporting the instrument carriage. The base flow (q_0) was 0.02 m^3/s, initial water depth (h) was 0.0544 m, and shear velocity of u^* = 0.031 m/s, determined for the condition of incipient motion of sediment with d_{50} = 0.001 m. Yen conducted five experimental runs, each running with the same initial sediment size gradation but varying discharges for each experiment. The maximum discharge was limited to 0.075 m^3/s.

Table 2. Representative size classes of initial bed material.

Size Class	1	2	3	4	5	6	7	8
Grain size (mm)	8.52	4.76	3.36	2.00	1.19	0.84	0.42	0.25
Fraction (%)	5.0	5.0	14.0	18.0	18.0	25.0	10.0	5.0

The bed elevations, corresponding changes, and transverse sediment sorting were measured and investigated after each experiment at different bend sections. The experiment result showed that the maximum scour and deposition occur at higher hydrograph discharges. In run number 4, the maximum deposition occurred near the inner bank at a 90° bend section, and the maximum scour occurred at a 180° bend section. It was also mentioned that the sediment was finer in the inner bank and coarser near the outer bank for higher discharges.

In this study, the experimental run number 4 is chosen to validate the proposed morphodynamic model systems. It has a maximum discharge of 0.053 m^3/s at 100 min and total runoff time of 300 min. Figure 7 shows the corresponding triangular-shaped hydrograph with rising and falling limbs.

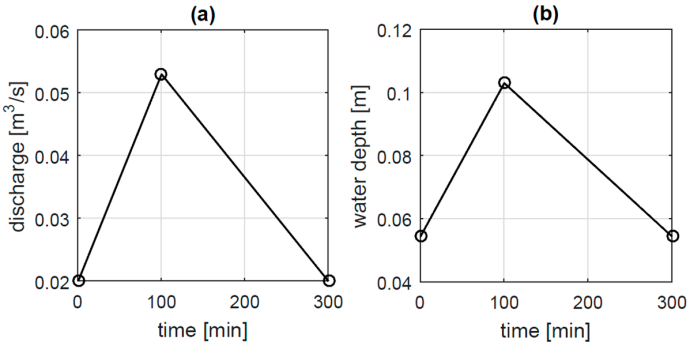

Figure 7. (**a**) Inflow hydrograph and (**b**) outflow water depth of experiment number 4 conducted by Yen [28].

4. Model Application

4.1. Model Evaluation

According to Legates [37], the model performance evaluation should include at least one goodness-of-fit or relative error measure (e.g., coefficient of determination (R^2)) and at least one absolute error measure (e.g., root mean square (RMSE) or mean absolute error (MAE)). In this paper, the model performance is evaluated based on the values of R^2, RMSE, and MAE, which are determined using the following equations:

$$R^2 = 1 - \frac{\sum_{i=1}^{n}\left([\Delta z/h_0]_{i(measured)} - [\Delta z/h_0]_{i(simulated)}\right)^2}{\sum_{i=1}^{n}\left([\Delta z/h_0]_{i(measured)} - [\Delta z/h_0]_{i(mean)}\right)^2} \quad (1)$$

$$RMSE = \sqrt{\frac{1}{n}\sum_{i=1}^{n}\left([\Delta z/h_0]_{i(measured)} - [\Delta z/h_0]_{i(simulated)}\right)^2} \quad (2)$$

$$\mathrm{MAE} = \frac{1}{n}\sum_{i=1}^{n}\left|[\Delta z/h_0]_{i(measured)} - [\Delta z/h_0]_{i(simulated)}\right| \quad (3)$$

where $\Delta z/h_0$ is the ratio of bed level change to initial depth, the suffixes measured and predicted denote the measured values from the Yen experiment and predicted values from the model, respectively. R^2 indicates the degree of similarity between measured and predicted values and determines how well considered independent variables account for the variance of the measured dependent variable. Higher values correlate with more significant model predictive capability, and R^2 values close to 1 indicate that the measured and predicted values are very similar [38]. The RMSE computes the square error of the prediction compared to actual values and calculates the square root of the summation value. The RMSE is the average distance of a data point from the fitted line measured along a vertical line. In contrast to the RMSE, the mean absolute error (MAE) is a quantity used to measure how close predictions are to the measured outputs. The MAE computes the average magnitude of error between predicted and actual values with no distinction between error directions. Low RMSE and MAE values indicate high confidence in the model-predicted values [37].

4.2. Model Calibration

In the experiment, the evolution of the bed in a 180° channel bend was investigated under unsteady-flow conditions with non-uniform sediment where the hydromorphological model systems have been validated against laboratory experiment. When coupling the sediment transport module with 2D flow models there are various calibration parameters that need to be parameterized for each model. Here, the bed-load transport formula is a vital calibration parameter that must be defined for models. As a result, the method of Engelund–Hansen [39] has been applied for the HYDRO-FT model, while TELEMAC applies the Meyer–Peter and Müller (MPM) formula [40] with a bed-load factor of 12 to simulate the laboratory experiment number 4 of Yen and Lee [28]. In the case of the BASEMENT modeling system, formulae by Hunziker [41] and Wu [42] have given good calibration results. With the same active layer thickness, prediction of the Hunziker formula is better for the scour side, while it overestimated on the deposit side. This result was exactly the opposite for the Wu formula [42], but the overestimation of deposition was in a permissible range. After multiple calibrations, the Wu formula [42] with bed-load factor 5 provided the most precise results.

The critical Shield's parameter values for the HYDRO-FT, TELEMAC, and BASEMENT models are defined as 0.03, 0.04, and 0.03, respectively. The bed roughness was taken for the TELEMAC model as approximately three times the mean diameter, ks = 0.0035 m. The BASEMENT model applies the friction value of 40 $m^{1/3}/s$ for Strickler's coefficient. For the case of HYDRO-FT, after a trial and error procedure, it was found that defining three different types of materials for the main channel and inner and outer banks can significantly improve the accuracy of the model performance. As a result, the calibrated manning bed roughness values for corresponding sections are obtained as 0.025, 0.022, and 0.028, respectively. The non-cohesive bed porosity of 0.25, 0.37, and 0.37 are considered for the TELEMAC, HYDRO-FT, and BASEMENT models, respectively. A very important feature available in the TELEMAC model is the option to consider the effect of secondary transverse currents on sediment transport rates. The method of Engelund [39] has been programmed to reproduce transverse bed evolution in curved channels. The bottom shear stress direction and magnitude are modified depending on the water depth h and the radius of curvature r. The radius, unknown in the model, can be substituted using the formulation for the slope of the free surface, $\partial Z_s/\partial n$, in bends as:

$$g(\partial Z_s/\partial n) = \alpha U^2/r \quad (4)$$

where Z_s is the free surface elevation and n is the transverse direction.

The correction factor α is the only calibration parameter and should be set as 0.75 in the presence of bedforms and as 1 for flatbed conditions. The value of 0.75 was chosen as the calibrated secondary currents alpha coefficient in this part. This parameter is not available in the same format in the

HYDRO-FT and the BASEMENT software. In these models, the bed shear stress deviation δ_r from the mean flow direction can be roughly determined with the following equation [35,43]:

$$\tan \delta_r = -Ah/r \tag{5}$$

where coefficient A is a calibratable parameter normally ranging between 8 and 12. The value of 12 was chosen in this case for the HYDRO-FT model. The radius of curvature r is derived from local changes in the flow direction. For the BASEMENT model, after multiple calibration procedures the best value of the curvature transport factor was selected as 9.

Another crucial factor necessary for calculating bed-load sediment transport rates for each class of sediment is the effect of hiding exposure. That means that in a sediment mixture, bigger particles will be more exposed to the flow than the smaller ones, and therefore prediction of sediment transport rates with classical sediment transport formulae must be corrected using a hiding exposure correction factor. Coupling the sediment transport module SISYPHE to TELEMAC allows the user to set the value of hiding factor for a particular size class and to choose a proper hiding factor formula. Two formulae, Egiazaroff [44] and Ashida and Michiue [45] were written based on the Meyer–Peter and Müller formula. Both formulae modify the critical Shield's parameter that will be used in the Meyer–Peter and Müller formula. Therefore, a useful combination is only attained with threshold formulae. The formula of Karim and Kennedy can be used in combination with any bed-load transport predictor. This formula directly modifies the bed-load transport rate. In this research, the hiding factors were initially calculated using the formulation of Egiazaroff, which is given as:

$$\zeta_i = \left[\frac{\log(19)}{\log(19 d_i/d_m)}\right]^2 \tag{6}$$

where the coefficient ζ_i is the hiding factor for the i-th sediment class size, d_i is the i-th sediment class size, and d_m is the mean sediment size.

After calculating the hiding factors using the above equation, some values were slightly changed during the calibration process to reproduce the most accurate simulation. Finally, the values of 6.0, 2.8, 1.45, 1.0, 0.29, 0.04, 0.01, and 0.01 were considered as suitable hiding factors for particular size classes. There is no option in the HYDRO-FT model to consider this feature. In the case of BASEMENT, the Wu formula [42] was applied, which assumes the hiding and exposure factors as functions of hidden and exposed probability. These factors are related to the size and gradation of bed material. They calculated the probabilities of grain d_g hidden and exposed by grain d_i by:

$$p_{hid,g} = \sum_{i=1}^{ng} \beta_i \frac{d_i}{d_g + d_i}, \quad p_{exp,g} = \sum_{i=1}^{ng} \beta_i \frac{d_g}{d_g + d_i} \tag{7}$$

where p_{hid}, and $p_{exp,g}$ are the total hiding and exposing probabilities. The critical dimensionless Shield's parameter for each grain class g can be calculated with the hiding and exposure factors ng and the Shield's parameter of the mean grain size $\theta_{cr,m}$ as:

$$\theta_{cr,g} = \theta_{cr,m}\left(\frac{p_{exp,g}}{p_{hid,g}}\right)^m \tag{8}$$

where θ_{cr}, is the critical dimensionless shield parameter for each grain class g. In BASEMENT's calibration, m is selected as −0.6.

The active layer thickness is another crucial parameter of the models, estimated by calibration and specified by the user. The active-layer thickness is evaluated by an appropriate empirical concept of the depth of bed material, which supplies material for bed-load transport and suspended sediment entrainment. Researchers have considered the active-layer thickness to be a function of dune height or

water depth. Throughout the previous decades, many new formulae have been proposed to calculate the active-layer thickness [46]. However, all formulae were derived differently, and a definition of the active-layer thickness based on physical processes in this layer has not yet been given. In the presented models, the active-layer thickness is assumed to be constant.

Table 3 summarizes some of the most important physical and mathematical parameters applied for calibration of each model. It should be considered that the calibration parameters that are available in one modeling system might not be available in the others. For example, as can be seen in Table 1, each modeling system uses a different turbulence model, and it is difficult to apply the same for all. On the other hand, each model is calibrated individually to reach its best performance, and then the best-calibrated results obtained from them are compared. For instance, for sediment transport modeling, the MPM is providing the best results for TELEMAC, while BASEMENT performs more precise using the Wu formula. In this case, if the Wu sediment transport model is applied in TELEMAC, its performance is compromised. Therefore, there is no consistency among the calibrated parameters.

Table 3. Comparison of parameters utilized for each model calibration.

Applied Methods and Parameters	**Modeling System**		
	TELEMAC-MASCARET	**HYDRO-FT**	**BASEMENT**
Hydrodynamic Model	Saint–Venant FE	SWE	Boussinesq
Turbulence Model	k-ε model	combination of an empirical viscosity and constant viscosity	Boussinesq eddy viscosity
Sediment Transport Model	MPM	Engelund–Hansen	Wu
Numerical Model	The optimum numerical scheme is automatically selected by the code (conservative scheme)	The second order explicit Runge–Kutta	Godunov type methods
Mesh	Unstructured	Unstructured	Unstructured
Shield's Parameter	0.04	0.03	0.03
Bed Friction Parameter	Strickler	Strickler	Manning
Bed porosity	0.25	0.37	0.37
Hiding/Exposure Factor	Applied	Not available	Not available
Secondary Currents Coefficient	0.75	12	9

5. Results and Discussion

According to [28], a scour region exists for $r/r_c > 1.0$ and a deposition region for $r/r_c < 1.0$, where r/r_c is the ratio of radial coordinate of channel bend to the radius of curvature along central line in the bend. Appreciable bed scour and deposition begin at about the 30° section and gradually reduce after the 180° section. The bed topographies are quite different among the five runs of experiments. The difference is due to the effect of the unsteady flow parameter. In their experiments, a close examination of the bed topographies and the longitudinal profiles reveals that the area of maximum deposition height is located between the 75° and 90° sections. Additionally, the area of maximum scour depth is between the 165° and 180° sections. For experiment run number 4, which is relevant for the present study, maximum deposition height and scour depth occur exactly at the 90° and 180° sections, respectively. The transverse bed profiles in these two areas should be of great interest to practicing engineers. The transverse bed profiles for the sections of maximum deposition and scour are shown in Figure 8 and Table 4 for all models. The figure and table indicate that the BASEMENT model perfectly simulates deposition in the 90° section, while other models have smaller deposition heights near the inner bank.

In this section, the scour depth is precisely simulated by HYDRO-FT at the outer bank, whereas the TELEMAC model performs better than the other models for $0.95 \leq r/r_c \leq 1.050$. According to Figure 8 and Table 4, at the 180° section the HYDRO-FT model outperforms the others in the simulation of deposition depth, while the TELEMAC model performs more accurately in calculating scour depth at the outer bank. Although the BASEMENT model does not produce very accurate results for this section, its performance is comparable to the two other models. Figure 8 and Table 4 also reveal that the point of no change in bed elevation (i.e., $\Delta z/h_0 = 0$) generally shifts toward the inner bank, whereas it shifts, for all models, towards the outer bank.

The results of the goodness of fit for each model are shown in Table 5. According to this table, it can be generally concluded that at the 90° section the BASEMENT model provides the best efficiency with the highest value of $R^2 = 0.9970$ and the lowest RMSE = 0.0763 and MAE = 0.0613. For the 180° section the results are a little more complicated, where from RMSE and MAE viewpoints the TELEMAC model shows the best performance, while regarding R^2 BASEMENT performs best.

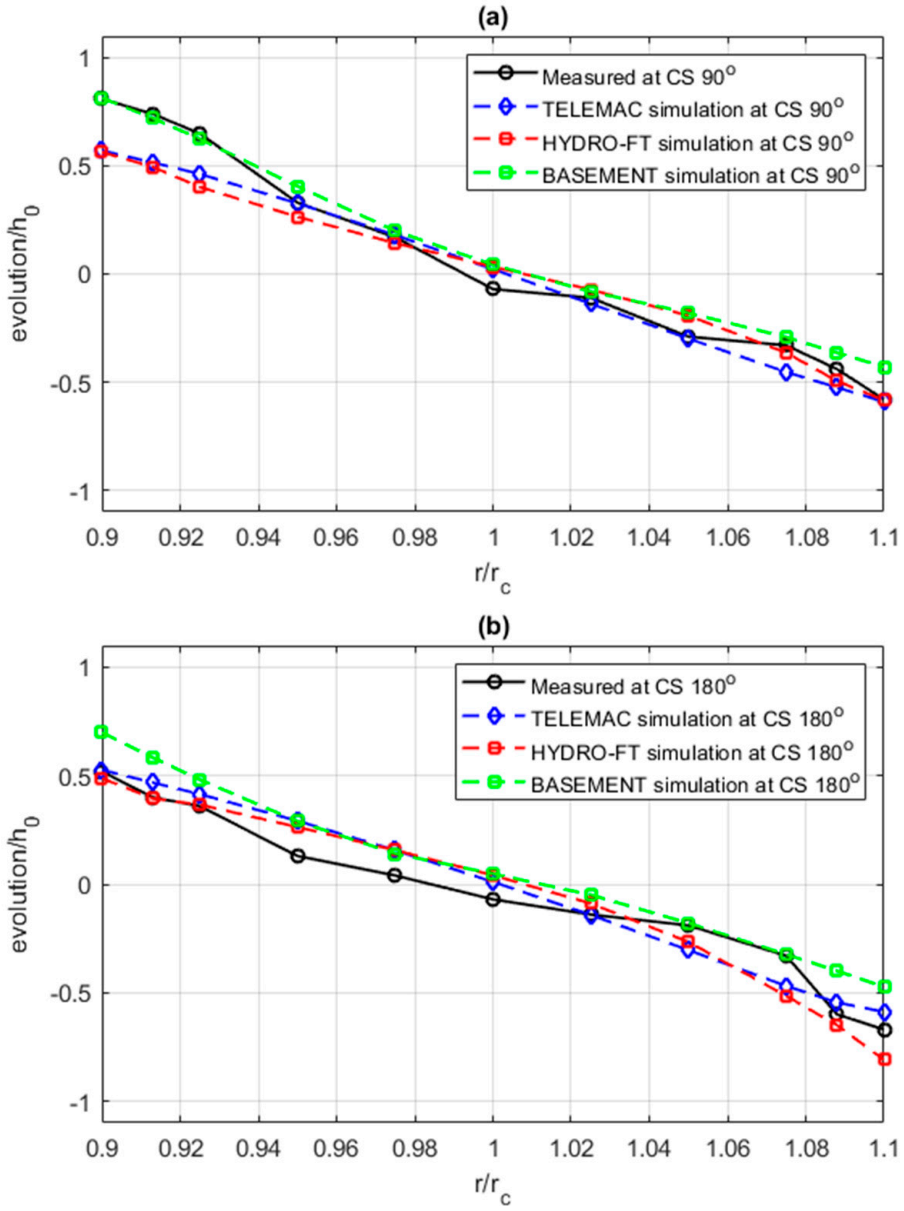

Figure 8. Comparison between measured and simulated bed evolutions normalized by the initial water depth after 5 h: (**a**) at the 90° cross-section; and (**b**) at the 180° cross-section.

Table 4. Transverse variation of non-dimensional bed deformation $\Delta z/h_0$ at sections of maximum deposition and scour (90° and 180° sections).

Model	r/r_c at 90° Section										
	0.900	**0.913**	**0.925**	**0.950**	**0.975**	**1.000**	**1.025**	**1.050**	**1.075**	**1.088**	**1.100**
Yen and Lee	0.810	0.740	0.650	0.330	0.170	−0.070	−0.110	−0.290	−0.330	−0.440	−0.580
BASEMENT	0.812	0.720	0.623	0.404	0.198	0.041	−0.080	−0.178	−0.290	−0.360	−0.420
TELEMAC	0.571	0.516	0.463	0.327	0.180	0.022	−0.137	−0.298	−0.450	−0.525	−0.590
HYDRO-FT	0.563	0.495	0.402	0.264	0.142	0.033	−0.072	−0.193	−0.364	−0.497	−0.584
Model	r/r_c at 180° Section										
	0.900	**0.913**	**0.925**	**0.950**	**0.975**	**1.000**	**1.025**	**1.050**	**1.075**	**1.088**	**1.100**
Yen and Lee	0.520	0.400	0.360	0.130	0.040	−0.070	−0.140	−0.190	−0.330	−0.600	−0.670
BASEMENT	0.695	0.580	0.478	0.288	0.140	0.047	−0.048	−0.178	−0.320	−0.398	−0.470
TELEMAC	0.526	0.468	0.415	0.292	0.156	0.010	−0.141	−0.303	−0.469	−0.545	−0.588
HYDRO-FT	0.488	0.395	0.367	0.263	0.157	0.041	−0.088	−0.266	−0.515	−0.650	−0.809

Table 5. Statistical performance of each model at 90° and 180° sections.

Model	Section 90°			Section 180°		
	R2	**RMSE**	**MAE**	**R2**	**RMSE**	**MAE**
TELEMAC	0.9810	0.1260	0.0920	0.9770	0.0934	0.0800
HYDRO-FT	0.9790	0.1290	0.0959	0.9710	0.1090	0.0947
BASEMENT	0.9970	0.0763	0.0613	0.9860	0.1399	0.1238

Figure 9a, Figure 10a, and Figure 11a show in plan-view a comparison of the bed level changes normalized by the initial water depth after 5 h between the laboratory experiment (isolines in black) and the TELEMAC, HYDRO-FT, and BASEMENT morphological models (colors), respectively. As can be seen from these figures, deposition and scour commence at about the 30° section, which is precisely modeled by TELEMAC and HYDRO-FT. The BASEMENT model, however, has simulated deposition long before this section and at the straight part of the channel. This unexpected deposition in the straight part of the channel can be observed throughout the whole simulation time. This could be due to computational errors or human-induced errors. In general, it can be observed that simulated results of BASEMENT shows better resemblances at the inner bank of the 90° bend section in comparison with the TELEMAC and the HYDRO-FT models. Around the center of curvature of the bend, TELEMAC has a better approximation, whereas HYDRO-FT has a better prediction in the outer bank of the 90° bend section. For the 180° bend, at both outer and inner banks, BASEMENT shows an overestimation of bed level change. Overall, at the 180° bend section, TELEMAC has a better approximation.

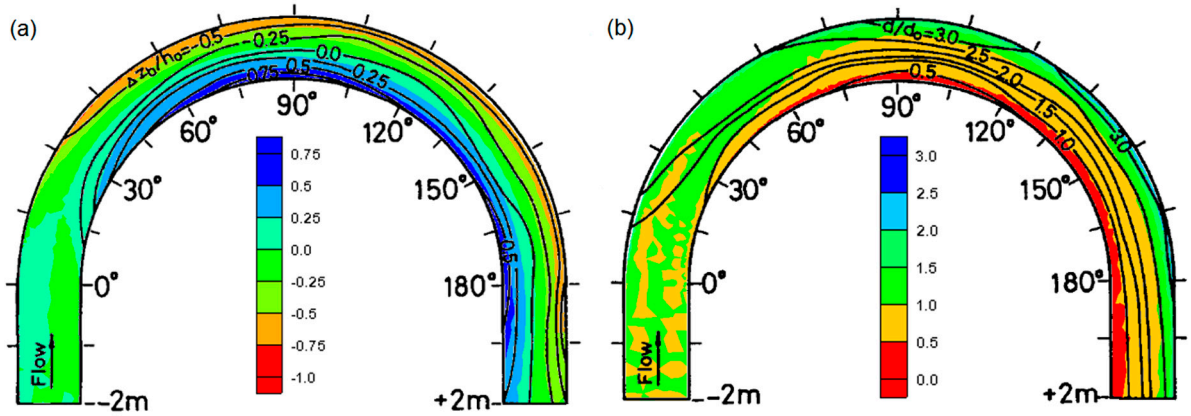

Figure 9. Measured (isolines) and TELEMAC calculated (colored) contours: (**a**) bed evolutions normalized by the initial water depth (h_0 = 0.0544 m); (**b**) median sediment size normalized by the initial median diameter.

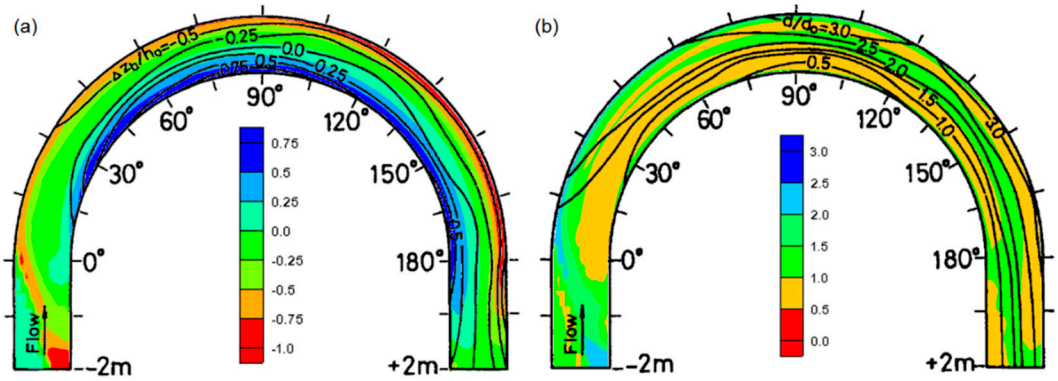

Figure 10. Measured (isolines) and HYDRO-FT calculated (colored) contours: (**a**) bed evolutions normalized by the initial water depth (h_0 = 0.0544 m); (**b**) median sediment size normalized by the initial median diameter.

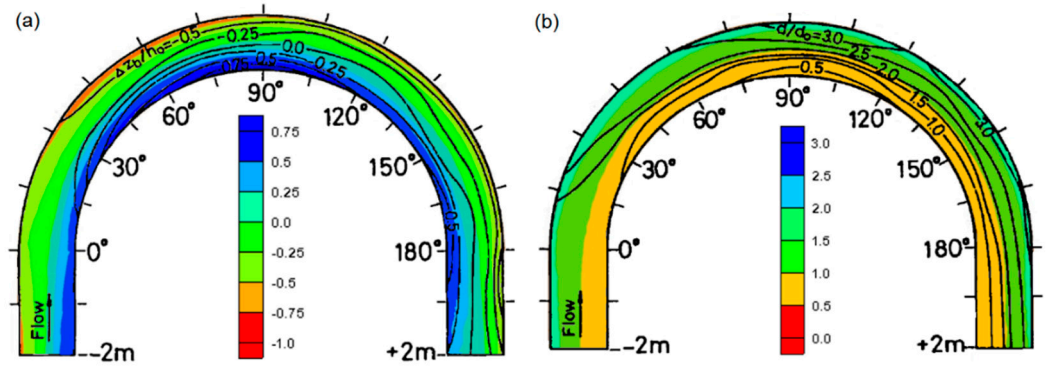

Figure 11. Measured (isolines) and BASEMENT calculated (colored) contours: (**a**) bed evolutions normalized by the initial water depth (h_0 = 0.0544 m); (**b**) median sediment size normalized by the initial median diameter.

The distribution of the measured (isolines in black) and calculated (colors) mean grain size using each model at the end of the experiment are also plotted in Figure 9b, Figure 10b, Figure 11b. Experimental results reveal that the largest variation of d/d_0 in the transverse direction occurred near the 90° section, indicating that the most intensive transverse sorting is in this area. The minimum and maximum measured d/d_0 values are 0.7 and 2.89, respectively, occurring in the inner and outer banks. The simulated d/d_0 values using the TELEMAC, HYDRO-FT, and BASEMENT models are in the range of 0.2–2.3, 0.5–2.48, and 0.3–2.1, respectively. According to the figures and the range of simulated d/d0 values, the models are not able to accurately predict the mean grain size distribution in the channel bend. Among the models, BASEMENT shows the lowest efficiency. Although the range of simulated d/d0 by the HYDRO-FT model is closer to the measured values, it can be seen from the figure that the predicted values are found in wrong locations. Generally, it can be concluded that the TELEMAC model is more accurate than the two other models in this case.

6. Conclusions

In the present study, three comprehensive morphodynamic modeling systems, namely TELEMAC-MASCARET, HYDRO-FT, and BASEMENT, were utilized to calculate flow and sediment transport in a curved alluvial channel. The models were applied to calculate the sediment sorting and the bed deformation under unsteady flow conditions with non-uniform materials. The predictions have been compared with data from the laboratory measurements and prototype observations of [28]. The actual limitations of the morphodynamic model are due to the high degree of empiricism, an inherent feature of most sediment transport models. As a result, there has been significant effort

aimed at reducing the uncertainty in the morphodynamic model results. After an extensive model calibration process, it has been concluded that all models are able to predict the deposition and scour in the channel bend accurately. The simulated results showed that at the inner bank of the 90° bend section BASEMENT performed better, while around the center of the bend curvature TELEMAC had a better approximation. The HYDRO-FT showed a better prediction in the outer bank of the 90° bend section. Moreover, at the 180° bend section, TELEMAC provided a better approximation, while BASEMENT overestimated the bed level changes. In contrast the calculation of the bed topographies and the longitudinal profiles, the models are not able to accurately predict the mean grain size distribution in the channel bend. However, it could be concluded that the TELEMAC model was more accurate than the two other models in this case.

Author Contributions: K.K., S.L., M.R., T.L., and N.D.N. designed the study, processed and analyzed the data. K.K. and S.L. developed the models, interpreted the results and wrote the paper. M.R., T.L., and N.D.N., assisted also in the data analysis. The study has been carried out together by M.D.B., and P.R., who contributed to the model development stage with theoretical considerations and practical guidance, assisted in the interpretations and integration of the results and helped in preparation of this paper with proof reading and corrections.

Funding: This research was funded by Bayerisches Staatsministerium für Umwelt und Verbraucherschutz.

Conflicts of Interest: The authors declare no potential conflict of interest.

References

1. Exner, F.M. Über die wechselwirkung zwischen wasser und geschiebe in flussen. *Akad. Wiss. Wien Math. Naturwiss. Klasse* **1925**, *134*, 165–204.
2. Graf, W.H. *Hydraulics of Sediment Transport*; McGraw-Hill: New York, NY, USA, 1971; pp. 287–291.
3. Leliavsky, S. *An Introduction to Fluvial Hydraulics (No. 627.12 L45)*; Dover Publications: Mineola, NY, USA, 1955.
4. Raudkivi, A.J. *Loose Boundary Hydraulics*; Pergamon: Oxford, UK, 1967; pp. 176–177.
5. Yang, C.T. *Sediment Transport: Theory and Practice*; McGraw Hill: New York, NY, USA, 1996.
6. Kubatko, E.J.; Westerink, J.J.; Dawson, C. An unstructured grid morphodynamic model with a discontinuous Galerkin method for bed evolution. *Ocean Modeling* **2006**, *15*, 71–89. [CrossRef]
7. Long, W.; Kirby, J.T.; Shao, Z. A numerical scheme for morphological bed level calculations. *Coast. Eng.* **2008**, *55*, 167–180. [CrossRef]
8. Godunov, S.K. A difference method for numerical calculation of discontinuous solutions of the equations of hydrodynamics. *Mat. Sb.* **1959**, *89*, 271–306.
9. Roe, P.L. Approximate Riemann solvers, parameter vectors, and difference schemes. *J. Comput. Phys.* **1981**, *43*, 357–372. [CrossRef]
10. Nicholson, J.; Broker, I.; Roelvink, J.A.; Price, D.; Tanguy, J.M.; Moreno, L. Intercomparison of coastal area morphodynamic models. *Coast. Eng.* **1997**, *31*, 97–123. [CrossRef]
11. Mahbub Alam, M. Application of MacCormack Scheme to the Study of Aggradation-Degradation in Alluvial Channels. Master's Thesis, Bangladesh University of Engineering and Technology (BUET), Dhaka, Bangladesh, 1998.
12. Kassem, A.A.; Chaudhry, M.H. Numerical modeling of bed evolution in channel bends. *J. Hydraul. Eng.* **2002**, *128*, 507–514. [CrossRef]
13. Johnson, H.K.; Zyserman, J.A. Controlling spatial oscillations in bed level update schemes. *Coast. Eng.* **2002**, *46*, 109–126. [CrossRef]
14. Hudson, J.; Damgaard, J.; Dodd, N.; Chesher, T.; Cooper, A. Numerical approaches for 1D morphodynamic modeling. *Coast. Eng.* **2005**, *52*, 691–707. [CrossRef]
15. Khosronejad, A.; Kozarek, J.L.; Diplas, P.; Hill, C.; Jha, R.; Chatanantavet, P.; Heydari, N.; Sotiropoulos, F. Simulation-based optimization of in-stream structures design: Rock vanes. *Environ. Fluid Mech.* **2018**, *18*, 695–738. [CrossRef]
16. Khosronejad, A.; Sotiropoulos, F. Numerical Simulation of turbulent flow and sediment transport around real-life stream restoration structures. In Proceedings of the 64th Annual Meeting of the APS Division of Fluid Dynamics, Baltimore, Maryland, 20–22 November 2011.

17. Escauriaza, C.; Sotiropoulos, F. Initial stages of erosion and bedform development in a turbulent flow around a cylindrical pier. *J. Geophys. Res. Earth Surf.* **2011**, *116*. [CrossRef]
18. Roulund, A.; Sumer, B.M.; Fredsöe, J.; Michelsen, J. Numerical and experimental investigation of flow and scour around a circular pile. *J. Fluid Mech.* **2005**, *534*, 351–401. [CrossRef]
19. Kang, S.; Khosronejad, A.; Sotiropoulos, F. Numerical simulation of turbulent flow and sediment transport processes in arbitrarily complex waterways. In *Environmental Fluid Mechanics, Memorial Volume in Honour of Prof. Gerhard H. Jirka*; CRC Press: Boca Raton, FL, USA, 2012; pp. 123–151.
20. Khosronejad, A.; Flora, F.; Zhang, Z.; Kang, S. Large-eddy simulation of flood propagation and sediment transport in a dry-bed desert stream. *Int. J. Sed. Res.* **2019**. under review.
21. Sotiropoulos, F.; Khosronejad, A. Sand waves in environmental flows: Insights gained by coupling large-eddy simulation with morphodynamics. *Phys. Fluids* **2016**, *28*, 021301. [CrossRef]
22. HydroQual Inc. *User's Manual, Version 1.3*; HydroQual, Inc.: Mahwah, NJ, USA, 2002; p. 188.
23. Warren, I.R.; Bach, H. MIKE 21: A modeling system for estuaries, coastal waters, and seas. *Environ. Softw.* **1992**, *7*, 229–240. [CrossRef]
24. Lesser, G.R.; Roelvink, J.V.; van Kester, J.A.T.M.; Stelling, G.S. Development and validation of a three-dimensional morphological model. *Coast. Eng.* **2004**, *51*, 883–915. [CrossRef]
25. Warner, J.C.; Sherwood, C.R.; Signell, R.P.; Harris, C.K.; Arango, H.G. Development of a three-dimensional, regional, coupled wave, current, and sediment-transport model. *Comput. Geosci.* **2008**, *34*, 1284–1306. [CrossRef]
26. Latteux, B. Techniques for long-term morphological simulation under tidal action. *Mar. Geol.* **1995**, *126*, 129–141. [CrossRef]
27. van der Wegen, M.; Roelvink, J.A. Long-term morphodynamic evolution of a tidal embayment using a two-dimensional, process-based model. *J. Geophys. Res. Ocean.* **2008**, *113*. [CrossRef]
28. Yen, C.L.; Lee, K.T. Bed topography and sediment sorting in channel bend with unsteady flow. *J. Hydraul. Eng.* **1995**, *121*, 591–599. [CrossRef]
29. Hervouet, J.M. *Hydrodynamics of Free Surface Flows: Modeling with the Finite Element Method*; John Wiley & Sons: Hoboken, NJ, USA, 2007.
30. Villaret, C.; Huybrechts, N.; Davies, A.G.; Way, O. Effect of bed roughness prediction on morphodynamic modeling: Application to the Dee estuary (UK) and to the Gironde estuary (France). In Proceedings of the 34th World Congress of the International Association for Hydro-Environment Research and Engineering: 33rd Hydrology and Water Resources Symposium and 10th Conference on Hydraulics in Water Engineering, Brisbane, Australia, 26 June–1 July 2011; p. 1149.
31. DVWK. *DVWK Schriften—Heft Nr. 127: Numerische Modelle von Flüssen*; Seen und Küstengewässern: Bonn, Germany, 2000.
32. Nujic, M. *Praktischer Einsatz eines Hochgenauen Verfahrens für die Berechnung von Tiefengemittelten Strömungen*; Mitteilungen des Instituts für Wasserwesen der Universität der Bundeswehr München: München, Germany, 1999.
33. Abbott, M.B. *Computational Hydraulics, Elements of the Theory of Free-Surface Flows*; Pitman Publ.: London, UK, 1979.
34. Yörük, A.; Sacher, H. Methoden und Qualität von Modellrechnungen für HW-Gefahrenflächen. *Simul. Model. Wasserbau Wasserwirtsch.* **2014**, *50*, 55–64.
35. Rozovskii, I.L. *Flows of Water in Bends of Open Channels*; Academy of Sciences of the Ukrainian SSSR: Kiev, Ukraine, 1957.
36. Vetsch, D.; Rousselot, P.; Volz, C.; Vonwiller, L.; Peter, S.; Ehrbar, D.; Veprek, R. *System Manuals of BASEMENT, Version 2.4. Laboratory of Hydraulics, Glaciology, and Hydrology*; ETH Zürich: Zürich, Switzerland, 2014.
37. Legates, D.R.; McCabe, G.J., Jr. Evaluating the use of "goodness-of-fit" measures in hydrologic and hydroclimatic model validation. *Water Resour. Res.* **1999**, *35*, 233–241. [CrossRef]
38. Kaveh, K.; Bui, M.D.; Rutschmann, P. A comparative study of three different learning algorithms applied to ANFIS for predicting daily suspended sediment concentration. *Int. J. Sediment Res.* **2017**, *32*, 340–350. [CrossRef]
39. Engelund, F.; Hansen, E. *A Monograph on Sediment Transport in Alluvial Streams*; Technical University of Denmark: Copenhagen, Denmark, 1973.

40. Meyer-Peter, E.; Müller, R. Formulas for bed-load transport. In *IAHSR 2nd Meeting, Stockholm, Appendix 2*; IAHR: Madrid, Spain, 1948.
41. Hunziker, R.P. Fraktionsweiser Geschiebetransport. Ph.D. Thesis, ETH Zürich, Zürich, Switzerland, 1995.
42. Wu, W.; Wang, S.S.; Jia, Y. Non-uniform sediment transport in alluvial rivers. *J. Hydraul. Res.* **2000**, *38*, 427–434. [CrossRef]
43. Bridge, J.S. A revised model for water flow, sediment transport, bed topography and grain size sorting in natural river bends. *Water Resour. Res.* **1992**, *28*, 999–1013. [CrossRef]
44. Egiazaroff, I.V. Calculation of non-uniform sediment concentrations. *J. Hydraul. Div.* **1965**, *91*, 225–247.
45. Ashida, K.; Mishiue, M. Studies on bedload transport rate in alluvial streams. *Trans. JSCE* **1972**, *4*, 122–123.
46. Bui, M.D.; Rutschmann, P. Numerical modelling of non-equilibrium graded sediment transport in a curved open channel. *Comput. Geosci.* **2010**, *36*, 792–800. [CrossRef]